

Article

Adsorption of Sodium of Polyaspartic Acid on Serpentine and Its Effects on Selective Pyrite/Serpentine Flotation

Xihui Fang ^{1,2,*}, Guanfei Zhao ^{1,2,*}  and Yu Zhang ²

¹ Jiangxi Province Key Laboratory of Mining Engineering, Jiangxi University of Science and Technology, Ganzhou 341000, China

² School of Resource and Environment Engineering, Jiangxi University of Science and Technology, Ganzhou 341000, China

* Correspondence: 9120010014@jxust.edu.cn (X.F.); fly.guan@163.com (G.Z.)

Abstract: Due to the optimum dissolution of the hydroxyl ion, serpentine is positively charged and tends to cover the sulfide mineral surface as a slime coating through electrostatic attraction, which intensively worsens sulfide flotation. To handle this problem, the sodium of polyaspartic acid (PASP) was employed as the selective depressant for the flotation of pyrite from serpentine in this work. Micro-flotation results showed that the fine serpentine of $-10\ \mu\text{m}$ could intensively hinder pyrite flotation, with a maximum decrease of about 75.8% in pyrite recovery at pH 9. However, at this pH, pyrite recovery remarkably increased from 20.17% to 92.68% when 15 mg/L PASP was introduced. Zeta potential results depicted that the addition of PASP overcompensated the positive charge on the serpentine surface and rendered it negative, while it had little impact on that of pyrite. Hence, the hetero-coagulation between serpentine and pyrite was broken due to the electrostatic repulsion, which was further confirmed by turbidity results. After that, the adsorption of PAX on the pyrite surface was restored, and the selective flotation of pyrite from serpentine was obtained. XPS analyses revealed that the chelation interaction between the carboxylate groups in PASP and the magnesium cations that remained on the serpentine surface were the main driving forces for the adsorption of PASP on the serpentine surface.

Keywords: pyrite; serpentine; PASP; chelation adsorption; flotation separation



Citation: Fang, X.; Zhao, G.; Zhang, Y. Adsorption of Sodium of Polyaspartic Acid on Serpentine and Its Effects on Selective Pyrite/Serpentine Flotation. *Minerals* **2022**, *12*, 1558. <https://doi.org/10.3390/min12121558>

Academic Editor: Wengang Liu

Received: 12 November 2022

Accepted: 28 November 2022

Published: 2 December 2022

Publisher's Note: MDPI stays neutral with regard to jurisdictional claims in published maps and institutional affiliations.



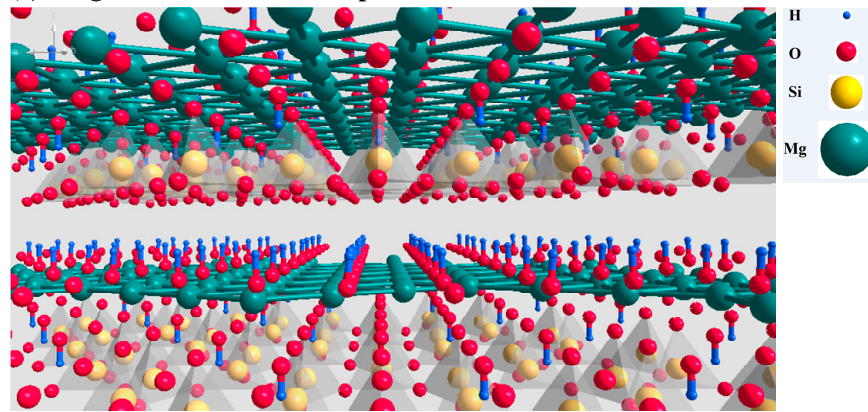
Copyright: © 2022 by the authors. Licensee MDPI, Basel, Switzerland. This article is an open access article distributed under the terms and conditions of the Creative Commons Attribution (CC BY) license (<https://creativecommons.org/licenses/by/4.0/>).

1. Introduction

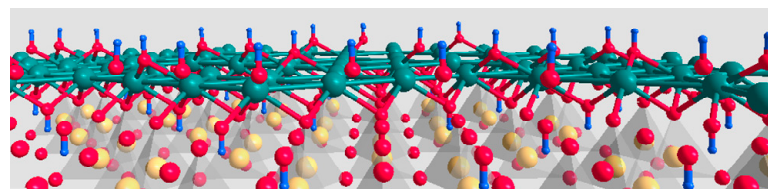
Serpentine (chemical formula, $\text{Mg}_6[\text{Si}_4\text{O}_{10}](\text{OH})_8$), a typical TO-type phyllosilicate mineral, which consists of alternating silicate tetrahedral sheets and brucite octahedral sheets (see Figure 1a) [1], normally exists in copper-nickel sulfide deposits as a gangue mineral. Examples would be the Jinchuan copper-nickel mine in the Gansu Province and the Yanbian copper-nickel mine in Sichuan Province [2,3]. At present, flotation, which is a separation process determined by the discrepancies between the affinity for water of the valuable sulfides and gangue minerals, is normally adopted to anteriorly obtained a high-quality concentrate before the smelting process [4,5]. Unfortunately, due to its low hardness, serpentine (Mohs hardness, 2.0) breaks easily and generates fines and slimes during the sulfide mineral beneficiation process [6,7]. Feng et al. [8] reported that the size fraction of serpentine slimes could reach $10\ \mu\text{m}$ in the Jinchuan copper-nickel concentrator. Under weakly alkaline flotation conditions, due to the preferential dissolution of the hydroxyl ion, serpentine slimes are normally positively charged due to the presence of residual magnesium cations on the (001) plane; it is considered the most common and stable cleavage surface of serpentine (see Figure 1b) [9]. Hence, these positive serpentine fines tend to attach to sulfide minerals as slime coatings due to their opposite surface charge [10]. The serpentine slimes on the surface of sulfide minerals significantly worsen the sulfide mineral flotation because these hydrophilic slimes will not only reduce the surface hydrophobicity of the valuable sulfide mineral but also hinder the interactions

between sulfide and the flotation reagent. To make matters worse, the serpentine slimes will enter into the concentrate through mechanical entrainment and improve the MgO content in the concentrate, which is unfavorable to the following smelting process [11,12].

(a) Magnesium surface of serpentine



(b) After the optimal dissolution of OH



(c) PASP

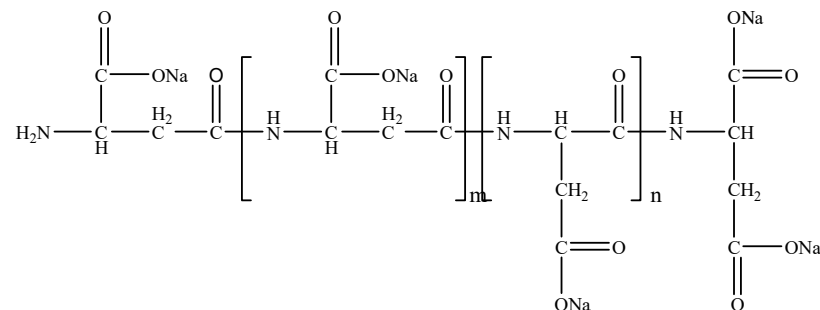


Figure 1. Crystal structures of (a) serpentine and (b) serpentine after optimal dissolution of hydroxyl ion, and (c) the molecular structure of PASP.

To date, the most commonly adopted approach for addressing the problem caused by the fines of serpentine on sulfide flotation is through adding chemical dispersants or depressants to selectively alter the surface charge properties of serpentine and the target sulfide mineral. Among these, sodium hexametaphosphate (SHMP) is one of the most normally used dispersant for reducing MgO content in the flotation concentrate in copper-nickel sulfide deposits involving serpentine, since it can selectively adsorb on the magnesium cations sites on the serpentine surface and also intensively improve the dissolution of Mg^{2+} , which alters the serpentine surface charge from positive to negative under weakly alkaline conditions [2,12–14]. Unfortunately, SHMP is a cyclic phosphate and easily decomposes in aqueous solutions, which limits its applications [15]. Sodium silicate is another common dispersant for eliminating the adverse impact of serpentine; it can change the surface charge of serpentine by adsorbing on its surface in the form of $\text{SiO}(\text{OH})_3^-$ [16,17]. However, the alteration efficiency of sodium silicate on serpentine is limited. Organic depressants such as carboxymethyl cellulose, starch, chitosan, guar gum, and their ramifications have also been reported to depress serpentine in nickel sulfide

flotation due to their multiple advantages, such as cheapness, non-toxicity, environmental friendliness, and so on [18,19]. However, the poor selectivity of these polysaccharides often caused some inevitable depression on the sulfide minerals of interest. Hence, it is of great importance to find a novel, clean reagent with a high selectivity for the efficient flotation separation of sulfide mineral from serpentine.

The sodium of polyaspartic acid (PASP, molecular structure see Figure 1c) is an environmental-friendly, biodegradable sodium polycarboxylate salt, which can be easily found in the shell of mollusks [20]. Since there are numerous carboxyl groups in its structure that can chelate with heavy metal ions [21], PASP has attracted wide attention in the fields of water treatment and corrosion inhibition [22]. In a flotation field, Wei et al. and Chen et al. [22,23] used polyaspartic acid to depress the flotation of Cu-activated sphalerite and calcite, respectively, and good flotation indices were obtained, since polyaspartic acid had a strong chelation ability towards copper and calcium ions. Furthermore, Liu et al. and Yang et al. [24,25] adopted PASP as a corrosion inhibitor for magnesium alloy, and these results confirmed that the PASP could intensively chelate with the Mg^{2+} on the alloy surface and form a soluble PASP–Mg complex. As we all know, the positive charge on serpentine under weakly alkaline conditions results from the prior dissolution of the hydroxyl ion with the residual positive magnesium ions on its surface [26]. Therefore, it can be speculated that PASP is also likely to be utilized as an efficient serpentine depressant in sulfide flotation. After that, the adsorbed PASP with a negative charge due to the dissociation of the Na ion will probably compensate the positive charge on the serpentine surface and consequentially, alleviate the hetero-coagulation between the sulfide and the serpentine. For all this, a rare report on the use of PASP as a selective depressant for the flotation separation of sulfide from serpentine was published, which is worth a deeper investigation.

This study explored the application potential of PASP to eliminate the adverse impact of serpentine on pyrite flotation in detail, and the inner actions were intensively discussed at pH 9, where the copper-nickel ore processing is usually performed [27]. It is worth mentioning here that since pentlandite crystals with high purities are hard to obtain, a typical sulfide mineral pyrite was selected as the target mineral in this work. The effect of PASP on the flotation separation of pyrite from serpentine was studied through micro-flotation tests, and its dispersion efficiency on the hetero-coagulation of pyrite and serpentine was evaluated by zeta potential experiments and turbidity measurements. Furthermore, the XPS technique was employed for exploring the adsorption mechanisms of PASP on serpentine, and adsorption experiments were finally conducted to study the adsorption behaviors of collectors on pyrite before and after the pretreatment of PASP.

2. Materials and Methods

2.1. Materials

The pure pyrite and serpentine samples were purchased from Daye, Hubei Province, and Donghai, Jiangsu Province, respectively. The crystal samples were crushed using a laboratory crusher to -1 mm, and then the crushed particles were hand ground to the wanted size using an agate mortar and pestle. In this work, the pyrite particle of 74 – 150 μm and serpentine samples with the size fractions of -10 μm , 38 – 74 μm , and 74 – 150 μm were adopted for the variety measurements, except for the zeta potential experiments, in which the used minerals particles were -2 μm . To detect the purity of mineral samples employed in this work, X-ray powder diffraction analyses were applied on pyrite and serpentine, and the XRD patterns obtained are shown in Figure 2. It can be seen that the pyrite sample possessed a high purity without any impurity peaks. The serpentine was also of high purity, with a trace amount of chlorite.

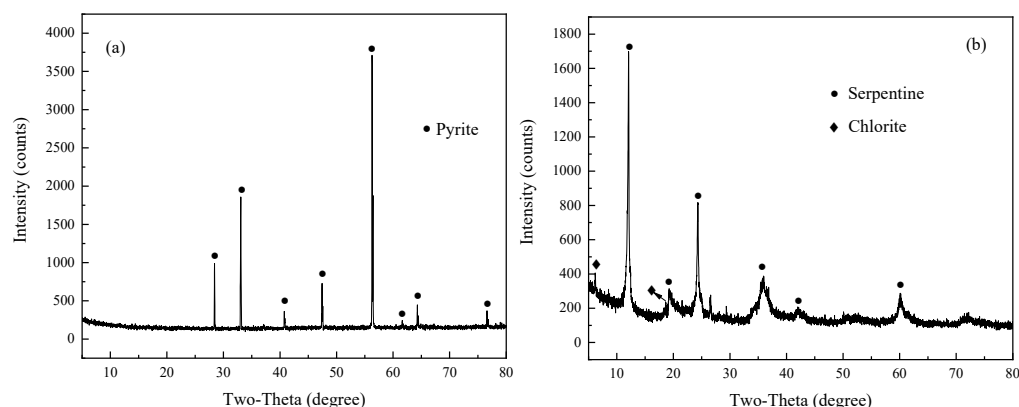


Figure 2. XRD patterns of (a) pyrite and (b) serpentine samples.

Analytical potassium amyl xanthate (PAX, purity > 97%) and methyl isobutyl carbinol (MIBC, purity > 99%) were used as the collector and the frother in this work, respectively, and both of them were commercially obtained from Shanghai Aladdin Biochemical Technology Co., Ltd. (Shanghai, China) The PASP (M.W, 7000–8000) of analytical grade purchased from Shanghai Macklin Biochemical Technology Co., Ltd. (Shanghai, China) was used as the depressant in this work. Sodium hydroxide (NaOH) and hydrochloric acid (HCl) of analytical grade were adopted as pH regulators, and distilled water was used for all the experiments in this work.

2.2. Experiments

2.2.1. Micro-Flotation Tests

Micro-flotation tests were performed through a laboratory XFG-type flotation machine (Jinlin Exploration equipment, Changchun, Jilin, China). For each test, 2 g of pyrite after a 3 min ultrasonic cleaning period for the removal of the oxide layer was mixed with 35 mL of distilled water in the flotation cell. According to the flotation conditions, a desired number of serpentine particles was added into the pulp. Then, the pulp was continuously stirred at 1992 rpm, and the pH regulators, PASP, and 8 mg/L PAX was added in order; the time interval between each reagent was 3 min. After that, 20 mg/L MIBC was added, and after 1 min of conditioning, the flotation was started. The total flotation time was 3 min, and both the overflowed and submerged solids were collected; their dried weights were used for calculating the flotation recovery of pyrite. The final data reported in this work originated from repeating the tests three times.

2.2.2. Zeta Potential Experiments

Zeta potential experiments were carried out to investigate the surface charges of pyrite and serpentine in the absence and presence of PASP. Firstly, 40 mg of mineral particles were dispersed into the 40 mL KCl solution of 1×10^{-3} mol/L in a 100 mL beaker. The pulp after pH adjustment was conditioned on a magnetic stirrer for 10 min at room temperature. After that, the pulp was settled for 5 min, and the liquid phase was then sucked out to detect the zeta potential of the minerals on a Malvern zeta potential analyzer (UK). The zeta potential for each mineral sample was detected three times; the average value and standard deviation were calculated and reported.

2.2.3. Turbidity Measurements

Turbidity measurements were also conducted in a KCl solution of 1×10^{-3} mol/L to maintain the stability of the mineral surface charge [28]. For each measurement, 1 g of pyrite and/or 0.1 g of serpentine particles was added into 100 mL KCl solution in the absence or presence of PASP in a 250 mL Erlenmeyer flask. After adjusting the pH, the pulp was stirred for 10 min to equilibrate the system. After 3 min of standing, the supernatant liquor of a fixed height (25 mL) was extracted for the turbidity detection [28]. The turbidity

tests were performed with a WGZ-3A scattering turbidimeter commercially obtained from Xin Rui instruments Co., Ltd., Shanghai, China, and each test was also triplicated.

2.2.4. X-ray Photoelectron Spectroscopy (XPS)

XPS, a commonly used technique to analyze surface chemical composition [29], was adopted for the investigation of the discrepancy in the surface chemical states between bare serpentine and the sample pretreated with PASP. To prepare the serpentine sample, 0.5 g of serpentine particles was added into 40 mL of distilled water or PASP solution in the flotation cell, and the suspension was then continuously agitated at pH 9 for 10 min. Then, the serpentine sample was obtained after filtering, rinsing, and drying below 40 °C in a vacuum drying chamber. XPS tests were performed on a K-Alpha-type ultrahigh vacuum electron spectrometer (Thermo Fisher, UK). The Thermo Avantage software was used in this work to fit the XPS spectra and describe the XPS core-level lines, and the C 1s peak at 284.8 eV was employed for calibration purposes.

2.2.5. Adsorption Experiments

The adsorption amount of PAX on the pyrite surface in the absence and presence of serpentine was investigated through the PAX reduction in solution before and after the conditioning. For each experiment, 1 g of pyrite and/or 0.1 g of serpentine solids were added into 100 mL of PAX solution of a different concentration in a conical flask. The mineral suspension was then stirred for 10 min after pH regulation. After that, the suspension was centrifuged, and a part of the liquid supernatant was pipetted out for the detection. The PAX concentration in the aqueous solution was determined with a Shimadzu UV-3000 ultraviolet spectrophotometer with the absorbance at 301 nm.

3. Results

3.1. Effects of PASP on the Selective Flotation of Pyrite from Serpentine

The detrimental influence of serpentine slimes on pyrite flotation performance was first researched through micro-flotation tests. Previous studies showed that the depression effect of serpentine on sulfide flotation was closely related to its size [30] and therefore, the effect of serpentine with different size fractions on the flotation performance of pyrite was researched as a function of serpentine concentration at pH 9, around where the beneficiation of copper-nickel sulfide ores were usually carried out [27]. These results are depicted in Figure 3.

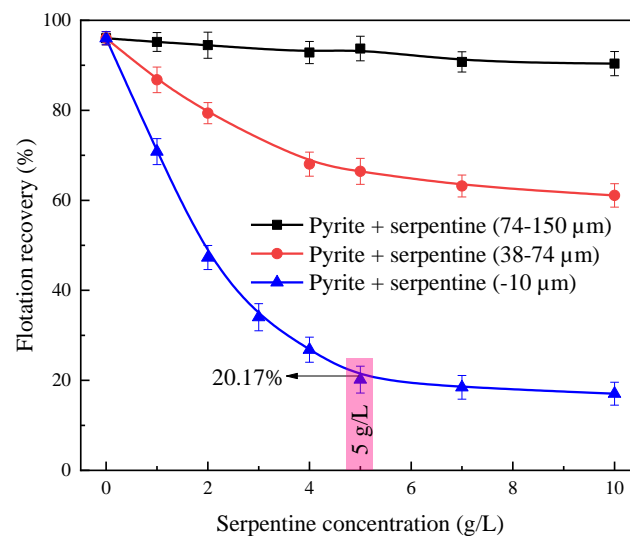


Figure 3. Effect of serpentine with different size fractions on pyrite flotation as a function of serpentine concentration (pH = 9).

As shown in Figure 3, the depression intensity of serpentine on pyrite floatability was strongly associated with its size fraction, and it can be concluded from Figure 3 that the finer the serpentine was, the stronger its depression on pyrite flotation was, which was in line with earlier reports [8,9]. When the $-10\ \mu\text{m}$ serpentine was introduced, it can be seen that pyrite recovery sharply decreased from 96.02% to 20.17% when the serpentine concentration increased from 0 to 5 g/L, verifying that serpentine slimes could strongly depress pyrite flotation [7]. As serpentine concentration was further increased, the decrease rate in pyrite recovery became very slow, and therefore, 5 g/L was used as the critical value for the added serpentine concentration in the following experiments. The serpentine with a size fraction of $-10\ \mu\text{m}$, which was close to the actual size in the Jinchuan copper-nickel concentrator [3], was used in the subsequential investigations.

In the presence of 5 g/L serpentine with a size fraction of $-10\ \mu\text{m}$, the effect of PASP on the selective flotation of pyrite from serpentine was investigated under different pulp pHs and PASP concentrations, and these results are presented in Figures 4 and 5, respectively.

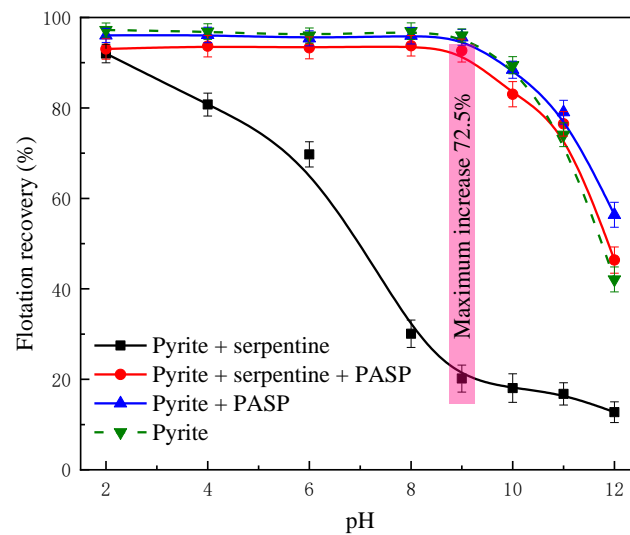


Figure 4. Effect of pulp pH on the flotation recovery of pyrite under different conditions ([PASP] = 15 mg/L, [serpentine ($-10\ \mu\text{m}$)] = 5 g/L).

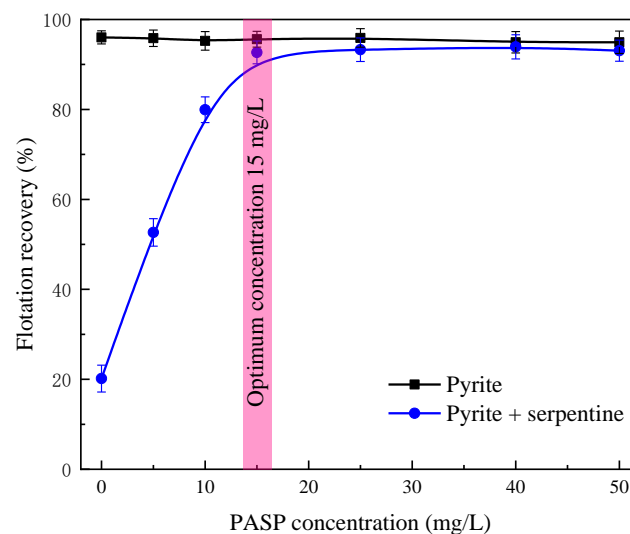


Figure 5. Effect of PASP on the flotation recovery of pyrite without and with serpentine ($-10\ \mu\text{m}$) as a function of PASP concentration (pH = 9, [serpentine] = 5 g/L).

Figure 4 exhibits the flotation behaviors of pyrite in the absence or presence of serpentine and PASP under different pulp pHs. It can be seen from Figure 4 that the floatability of bare pyrite was always higher than 90% in the pH range 2–10, while a significant drop in pyrite recovery could be found when the pH was above 10, which was due to the formation of iron oxide/hydroxide on its surface [21]. In addition, it can also be seen that the addition of PASP had little influence on the flotation of bare pyrite. However, in the presence of 5 g/L serpentine, the recovery of pyrite gradually decreased from 92.03% to 12.73% as the pH increased from 2 to 12 in the absence of PASP. Preceding studies indicated that this phenomenon resulted from the changing in the surface charge properties of minerals [10]. Sulfide ore flotation was normally conducted under weakly alkaline conditions around pH 9 [27], where the serpentine slimes possessed a intensive depression effect on pyrite flotation. Interestingly, the depression impact of fine serpentine on pyrite flotation was largely limited, and it can be seen from Figure 4 that a remarkable increase in pyrite recovery of about 72.5% could be achieved at pH 9 in the presence of serpentine when 15 mg/L PASP was introduced.

Figure 5 shows the flotation behaviors of pyrite in the absence and presence of serpentine ($-10\ \mu\text{m}$) under different PASP concentrations. Similar to the results listed in Figure 4, it is clear from Figure 5 that the bare pyrite flotation basically remained unchanged after adding PASP, with a recovery of around 95% in the entire PASP concentration range tested, from 0 to 50 mg/L. The addition of PASP could significantly reduce the inhibition of serpentine slimes on pyrite flotation. The recovery of pyrite remarkably increased from 20.17% to 92.68% as the PASP concentration increased from 0 to 15 mg/L; it remained stable even under a higher PASP concentration.

The results of micro-flotation tests demonstrated that PASP had an efficient depression influence towards serpentine and eliminated its adverse effect on pyrite flotation while possessing little impact on bare pyrite. Therefore, it can be speculated that PASP is likely to be applied as a selective flotation depressant for serpentine in sulfide flotation.

3.2. Effect of PASP on the Hetero-Coagulation between Pyrite and Serpentine

Since the electrostatic force was the main driving force for the hetero-coagulation between pyrite and serpentine [10], this section was carried out through zeta potential measurements to investigate the effect of PASP on the surface charge of minerals; its further influence on the aggregation/dispersion states of the pyrite/serpentine system was analyzed using turbidity tests.

Figure 6 lists the zeta potentials of pyrite and serpentine in the absence and presence of 15 mg/L PASP. It can be seen from Figure 6 that the isoelectric points of pyrite and serpentine without the employment of PASP were around 2.5 and 10.9, respectively, which was in line with previous reports [31,32]. At pH 9, the zeta potentials of pyrite and serpentine were $-38.26\ \text{mV}$ and $14.02\ \text{mV}$, respectively. Therefore, the hetero-coagulation between pyrite and serpentine was thought to happen because of their inverse surface charges. When 15 mg/L PASP was added into the system, the zeta potential of serpentine intensively decreased to the negative domain in the whole pH range detected, whereas the zeta potential of pyrite only decreased to a tiny extent, which suggested the adsorption intensity of PASP on serpentine was remarkably stronger than that on pyrite. Moreover, after the addition of PASP, both serpentine and pyrite were negatively charged at pH 9, and the electrostatic attraction between these two minerals might be transformed into electrostatic repulsion, which led to the removal of the serpentine slimes from the pyrite surface.

As we discussed in the introduction, the positively charged surface of serpentine at pH 9 was due to the magnesium cations that remained on its surface after the preferential dissolution of OH^- , which could offer the active sites the adsorption of PASP. However, according to the studies reported by past researchers [33,34], due to the semiconductor properties of sulfide minerals, the outmost surface of pyrite was probably composed of the iron oxide and/or hydroxide species during the flotation process, which could be

easily removed in the presence of PASP due to its strong chelation ability, and thus, the adsorption of PASP on the pyrite surface might be unfavorable. This might cause the difference between the adsorption behaviors of PASP on serpentine and pyrite, which can lead to the selective flotation of pyrite from serpentine.

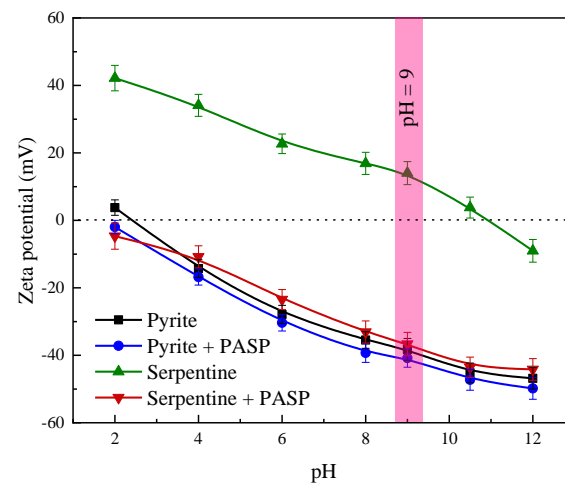


Figure 6. Effect of PASP on the zeta potentials of pyrite and serpentine under different pHs ([PASP] = 15 mg/L).

The turbidity can reveal the aggregation/dispersion states of mineral pulp. Therefore, a turbidity test was performed to study the influence of PASP on the dispersion state of the mixed pyrite/serpentine system. Figure 7 shows the turbidity of different mineral systems at pH 9. For a single mineral suspension, the turbidity of a single serpentine pulp was around 537 NTU, which was greatly higher than that of bare pyrite pulp, which possessed a value of about 20 NTU. When serpentine and pyrite were mixed with each other, a turbidity of around 420 NTU was obtained, which was far less than the sum of the turbidities for single serpentine and pyrite pulp, implying that a heterogeneous aggregation occurred between them. However, when PASP was employed, the turbidity of the mixed minerals pulp increased to 551 NTU, which suggested that the aggregation between serpentine and pyrite was destroyed, and a good dispersion state was achieved in the mixed minerals pulp. The turbidity results were in line with the zeta potential analyses.

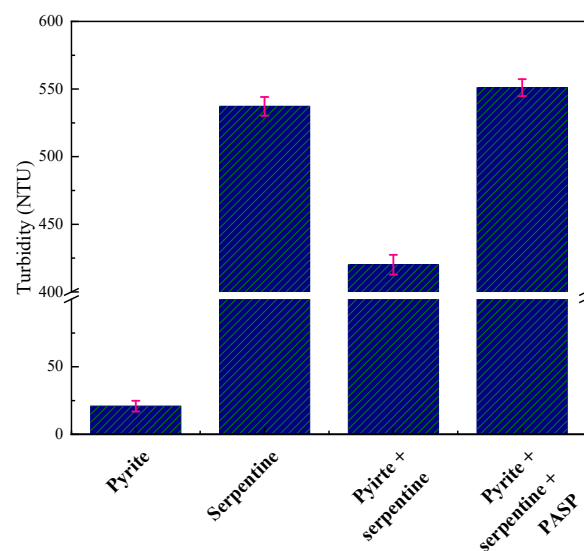


Figure 7. Turbidity of single pyrite and serpentine ($-10\ \mu\text{m}$) and their mixture in the absence and presence of PASP (pH = 9, [PASP] = 15 mg/L).

3.3. Adsorption Mechanisms of PASP on Serpentine Surface

The abovementioned contents illustrated that PASP selectively adsorbed on the serpentine surface and rendered its surface charge negative. However, the underlying adsorption mechanisms of PASP on the serpentine surface was still indistinct. Therefore, the XPS technique was used to investigate the adsorption mechanism of PASP on the serpentine surface in detail. The XPS spectra of serpentine before and after the pretreatment of PASP are shown in Figures 8 and 9.

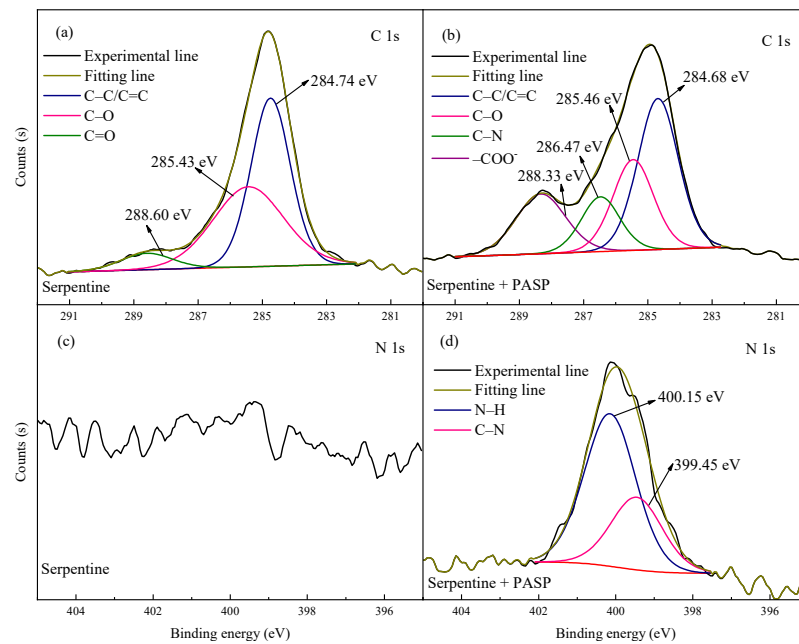


Figure 8. High-resolution spectra of (a,b) C 1s, and (c,d) N 1s of serpentine before and after the pretreatment of PASP (pH = 9).

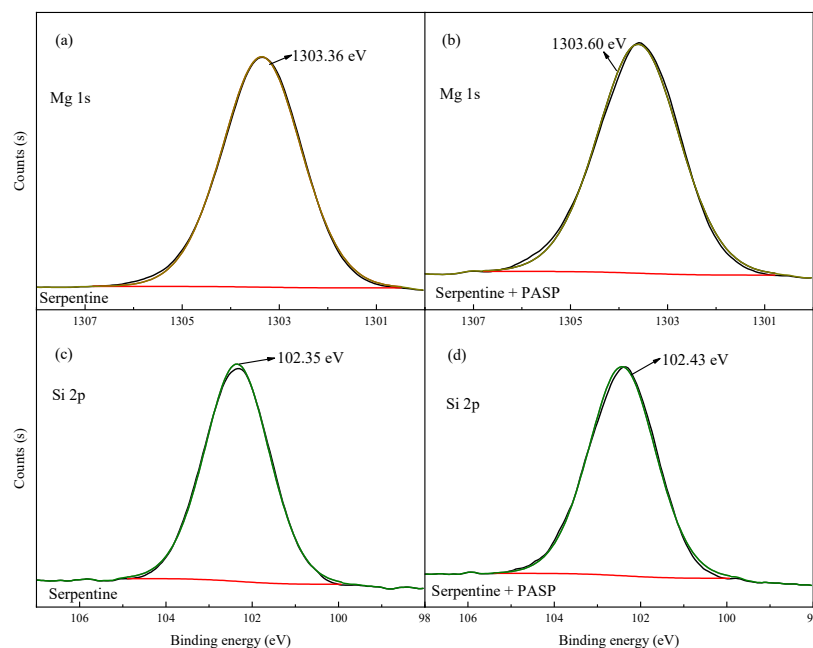


Figure 9. High-resolution spectra of (a,b) Mg 1s and (c,d) Si 2p of serpentine before and after the pretreatment of PASP (pH = 9).

The high-resolution XPS spectra of the C 1s and N 1s of serpentine before and after the pretreatment of PASP are presented in Figure 8. It can be seen from Figure 8a that the C 1s spectra of the bare serpentine surface could be fitted by three peaks around 284.8 eV, 285.4 eV, and 288.6 eV, which originated from the carbon atom in the forms of C–C, C–O, and C=O, respectively [35–37]. This was most likely due to organic contamination during the test process [38]. After the pretreatment of PASP, the intensity of the peak around 288.4 eV significantly increased, which might be caused by the adsorption of the carboxyl groups in PASP on the serpentine surface [36]. Furthermore, there was a new peak at 286.47 eV that appeared on the treated serpentine surface, which was caused by the C–N bond [39]. In addition, it is clear from Figure 8c that there were no obvious signals for the N 1s on the surface of the bare serpentine, suggesting that there was no N element on serpentine surface in the absence of PASP. However, after the pretreatment of PASP, a fresh peak generated, and this new peak could be deconvoluted into two peaks at 399.45 eV and 400.15 eV, which were due to the bonds of N–C and N–H, respectively [6,40]. These results illustrated that the adsorption of PASP on the serpentine surface took place at that time.

Figure 9 shows the changes in the high resolution XPS spectra of the Mg 1s and Si 2p of serpentine without and with the interaction of PASP. It is clear from Figure 9a,b that a positive shift of 0.24 eV (>0.2 eV) in the Mg 1s characteristic peaks could be found when serpentine was pretreated with PASP, which implied that the chemical environments of the magnesium cations on the serpentine surface was changed after the adsorption of PASP, and that this adsorption process was most likely chemical [41]. As shown in Figure 1c, there were large amounts of $-\text{COO}^-$ groups in the PASP structure after the decomposition of the sodium ion. Previous studies also confirmed that the carboxylate group can chelate with polyvalent metal ions via ionic linkages [9,42,43]. Therefore, these carboxylate radicals in the PASP might easily chemically adsorb on the serpentine surface through chelating with the magnesium cations exposed on the serpentine surface, thus altering its chemical state. In addition, it can also be seen from Figure 9c,d that the Si 2p spectra of serpentine depicted little variations before and after the pretreatment of PASP, indicating that PASP perhaps did not adsorb on the Si sites on the serpentine surface [44]. Therefore, it can be concluded from XPS analyses that PASP could chemically adsorb on the serpentine through the chelation interaction between its carboxylate radicals and the positive magnesium ions on the serpentine surface.

3.4. Influence of PASP on the Adsorption of Collector on Pyrite Surface

Previous studies indicated that the serpentine slime coatings on sulfide minerals could severely inhibit the adsorption of the xanthate collector on their surface, which is a key point for its deterioration impact on sulfide flotation [43]. Therefore, the effect of PASP on the adsorption behaviors of PAX on the pyrite surface in the presence of serpentine was studied at pH 9, and these results are listed in Figure 10.

It can be found from Figure 10 that the presence of serpentine intensively depressed the adsorption of PAX on the pyrite surface. Since that PAX basically did not adsorb on serpentine [6], which was also revealed by the pink line in Figure 10, the adsorption amount of PAX on serpentine was close to zero. Thus, it can be concluded that the remarkable decrease in the amount of adsorbed PAX on the pyrite surface resulted from the serpentine slime covering on the pyrite. Interestingly, the adsorption amount of PAX on the pyrite surface was regained to a great extent when 15 mg/L PASP was applied into the system, indicating that the employment of PASP could efficiently remove the serpentine slime from pyrite, which could confirm the results of the flotation, zeta potential, and turbidity experiments.

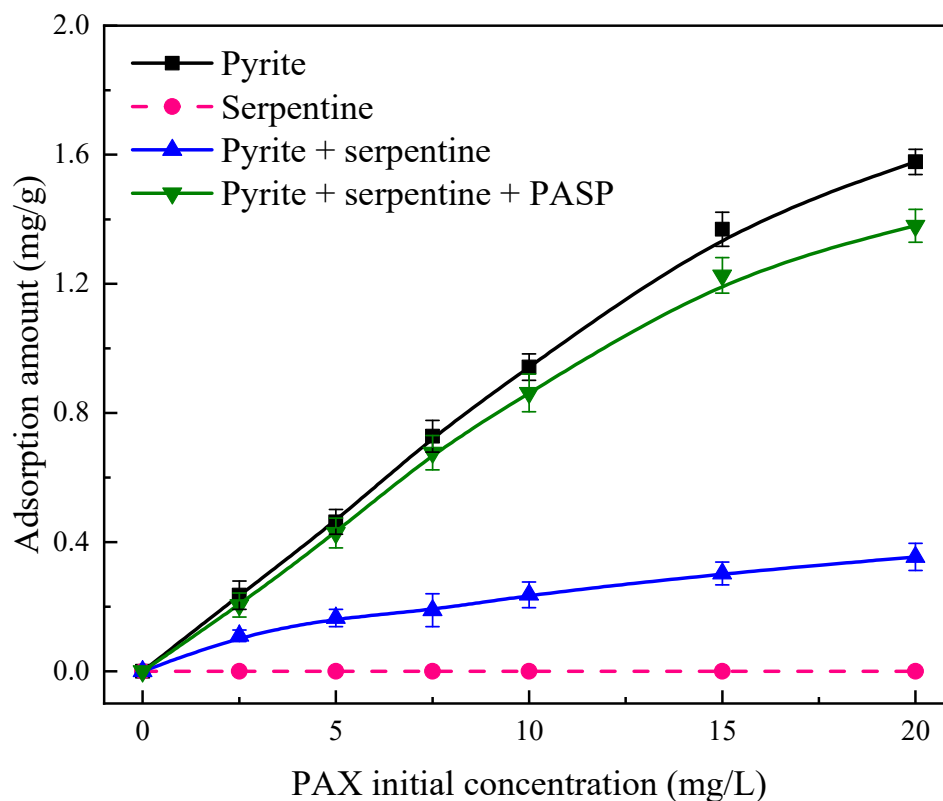


Figure 10. Adsorption amounts of PAX on the pyrite surface and serpentine ($-10\ \mu\text{m}$) under different conditions ($\text{pH} = 9$, $[\text{PASP}] = 15\ \text{mg/L}$).

4. Discussion

Based on all the experiments results listed above, a schematic diagram for explaining the influence of PASP on the selective flotation of pyrite from serpentine slimes is depicted in Figure 11. As shown in the magnesium surface of the serpentine structure at the bottom of Figure 11a, due to the preferential dissolution of the hydroxyl ion, the magnesium cations that remained on the serpentine surface led to its positively charged surface. Therefore, the hetero-coagulation between serpentine and pyrite commonly appeared during the flotation process due to their inverse surface charges. The serpentine slimes attached to the pyrite surface not only improve the surface hydrophilicity but also hindered the following PAX adsorption, which was presented by an orange sphere with a cyan edge in Figure 11a. Thus, pyrite flotation significantly deteriorated. When PASP was introduced (see Figure 11b), the carboxylate groups in its molecular structure could chelate with the residual magnesium cations on the serpentine surface and led to its adsorption on serpentine, as listed at the bottom of Figure 11b. Since there were large amounts of $-\text{COO}^-$ groups in its structure, PASP was negatively charged in the flotation pulp after ionization equilibrium. Hence, the positive charge on serpentine was overcompensated and rendered to negative after PASP adsorption. Electrostatic repulsion might happen because of the negative charges on the surfaces of both pyrite and serpentine. After that, the hetero-coagulation between these two minerals was destroyed, and the adsorption of PAX on the pyrite was regained, as shown in the upper half of Figure 11b. Therefore, the selective flotation of pyrite from serpentine was achieved with the application of PASP.

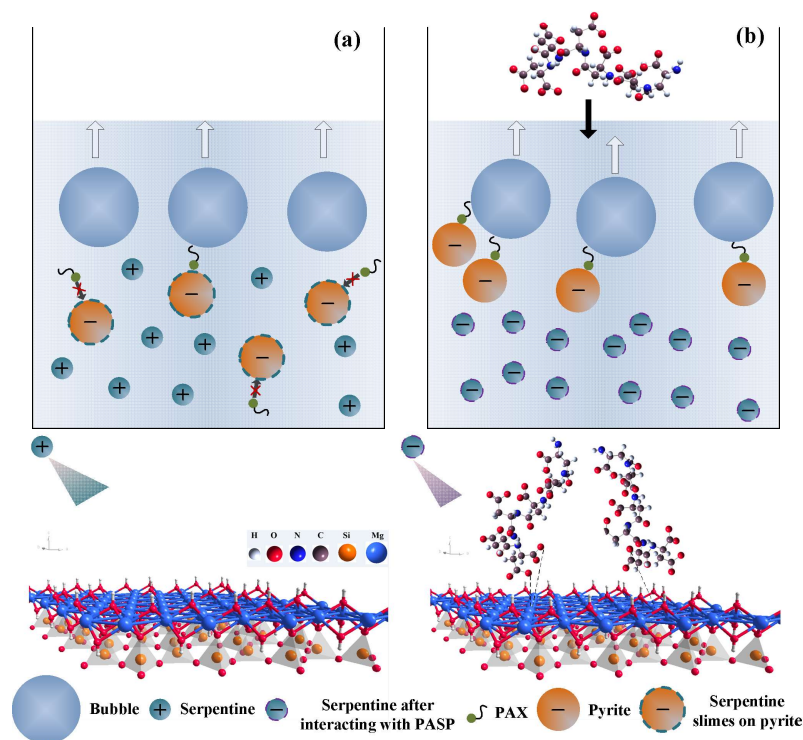


Figure 11. A schematic diagram of the flotation separation of pyrite from serpentine (a) in the absence of PASP and (b) in the presence of PASP.

5. Conclusions

In this research, PASP was adopted as a novel depressant for the selective flotation separation between pyrite and fine serpentine. According to the results and analyses of micro-flotation experiments, zeta potential tests, turbidity measurements, PAX adsorption, and XPS tests, the main conclusions can be drawn as follows:

(1) Fine serpentine ($-10\ \mu\text{m}$) tended to cover the pyrite surface and worsened its flotation terribly, especially under weakly alkaline conditions, where sulfide flotation commonly takes place. However, PASP could significantly limit the adverse impact of serpentine slimes on pyrite flotation, with a maximum increase of about 72.5% in pyrite recovery at pH 9.

(2) PASP could adsorb on serpentine through the chelation interaction between its carboxylate groups and the positive magnesium ions exposed on the serpentine surface, which resulted in the transformation of the serpentine surface charge from positive to negative. Meanwhile, PASP had little effect on the surface charge properties of pyrite, which was probably due to the outmost Fe-OOH layer of pyrite not being able to provide a stable adsorption site to PASP.

(3) The electrostatic repulsion between the negatively charged pyrite and serpentine destroyed the hetero-coagulation between them after the addition of PASP. Thus, the adsorption of PAX on the pyrite was regained, and the selective flotation of pyrite from serpentine was achieved.

Author Contributions: Conceptualization, X.F.; methodology, X.F., G.Z., and Y.Z.; formal analysis, X.F. and G.Z.; investigation, X.F.; resources, Y.Z.; data curation, X.F.; writing—original draft preparation, X.F. and G.Z.; writing—review and editing, X.F.; supervision, X.F.; funding acquisition, G.Z. All authors have read and agreed to the published version of the manuscript.

Funding: This research was funded by the Doctoral Research Foundation of Jiangxi University of Science and Technology [Grant number: 205200100631].

Data Availability Statement: The data presented in this study are available on request from the corresponding author. The data are not publicly available due to relevant further research is under way.

Conflicts of Interest: The authors declare no conflict of interest.

References

1. Hossain, F.M.; Dlugogorski, B.Z.; Kennedy, E.M.; Belova, I.V.; Murch, G.E. Ab-Initio Electronic Structure, Optical, Dielectric and Bonding Properties of Lizardite-1T. *Comput. Mater. Sci.* **2011**, *50*, 1725–1730. [\[CrossRef\]](#)
2. Zhao, K.; Yan, W.; Wang, X.; Wang, Z.; Gao, Z.; Wang, C.; He, W. Effect of a Novel Phosphate on the Flotation of Serpentine-Containing Copper-Nickel Sulfide Ore. *Miner. Eng.* **2020**, *150*, 106276. [\[CrossRef\]](#)
3. Feng, B.; Peng, J.; Zhang, W.; Luo, G.; Wang, H. Removal Behavior of Slime from Pentlandite Surfaces and Its Effect on Flotation. *Miner. Eng.* **2018**, *125*, 150–154. [\[CrossRef\]](#)
4. Chen, Y.; Guo, X.; Chen, Y. Using Phytic Acid as a Depressant for the Selective Flotation Separation of Smithsonite from Calcite. *Sep. Purif. Technol.* **2022**, *302*, 122104. [\[CrossRef\]](#)
5. Liu, D.; Zhang, G.; Chen, Y.; Huang, G.; Gao, Y. Investigations on the Utilization of Konjac Glucomannan in the Flotation Separation of Chalcopyrite from Pyrite. *Miner. Eng.* **2020**, *145*, 106098. [\[CrossRef\]](#)
6. Liu, D.; Zhang, G.; Huang, G.; Gao, Y.; Wang, M. The Flotation Separation of Pyrite from Serpentine Using Lemon Yellow as Selective Depressant. *Colloids Surf. A* **2019**, *581*, 123823. [\[CrossRef\]](#)
7. Liu, D.; Zhang, G.; Gao, Y. New Perceptions into the Detrimental Influences of Serpentine on Cu-Ni Sulfide Flotation through Rheology Studies and Improved the Separation by Applying Garnet. *Miner. Eng.* **2021**, *171*, 107110. [\[CrossRef\]](#)
8. Feng, B.; Lu, Y.; Luo, X. The Effect of Quartz on the Flotation of Pyrite Depressed by Serpentine. *J. Mater. Res. Technol.* **2015**, *4*, 8–13. [\[CrossRef\]](#)
9. Liu, D.; Zhang, G.; Chen, Y. Studies on the Selective Flotation of Pyrite from Fine Serpentine by Using Citric Acid as Depressant. *Miner. Eng.* **2021**, *165*, 106742. [\[CrossRef\]](#)
10. Bremmell, K.E.; Fornasiero, D.; Ralston, J. Pentlandite-Lizardite Interactions and Implications for Their Separation by Flotation. *Colloids Surf. A Physicochem. Eng. Asp.* **2005**, *252*, 207–212. [\[CrossRef\]](#)
11. Gao, Y.; Zhang, G.; Wang, M.; Liu, D. The Critical Role of Pulp Density on Flotation Separation of Nickel-Copper Sulfide from Fine Serpentine. *Minerals* **2018**, *8*, 317. [\[CrossRef\]](#)
12. Edwards, C.R.; Kipkie, W.B.; Agar, G.E. The Effect of Slime Coatings of the Serpentine Minerals, Chrysotile and Lizardite, on Pentlandite Flotation. *Int. J. Miner. Process.* **1980**, *7*, 33–42. [\[CrossRef\]](#)
13. Lu, Y.P.; Zhang, M.Q.; Feng, Q.M.; Long, T.; Ou, L.M.; Zhang, G.F. Effect of Sodium Hexametaphosphate on Separation of Serpentine from Pyrite. *Trans. Nonferrous Met. Soc. China* **2011**, *21*, 208–213. [\[CrossRef\]](#)
14. Feng, B.; Wang, P.; Lu, Y.; Feng, Q. Role of Sodium Hexametaphosphate in Flotation of A Nickel Ore. *Physicochem. Probl. Miner. Process.* **2016**, *52*, 170–181.
15. Rashchi, F.; Finch, J.A. Polyphosphates: A Review. Their Chemistry and Application with Particular Reference to Mineral Processing. *Miner. Eng.* **2000**, *13*, 1019–1035. [\[CrossRef\]](#)
16. Feng, B.; Lu, Y.; Feng, Q.; Li, H. Solution Chemistry of Sodium Silicate and Implications for Pyrite Flotation. *Ind. Eng. Chem. Res.* **2012**, *51*, 12089–12094. [\[CrossRef\]](#)
17. Feng, B.; Zhang, W.; Guo, Y.; Peng, J.; Ning, X.; Wang, H. Synergistic Effect of Acidified Water Glass and Locust Bean Gum in the Flotation of a Refractory Copper Sulfide Ore. *J. Clean. Prod.* **2018**, *202*, 1077–1084. [\[CrossRef\]](#)
18. Bicak, O.; Ekmekci, Z.; Bradshaw, D.J.; Harris, P.J. Adsorption of Guar Gum and CMC on Pyrite. *Miner. Eng.* **2007**, *20*, 996–1002. [\[CrossRef\]](#)
19. Zhang, C.; Liu, C.; Feng, Q.; Chen, Y. Utilization of N-Carboxymethyl Chitosan as Selective Depressants for Serpentine on the Flotation of Pyrite. *Int. J. Miner. Process.* **2017**, *163*, 45–47. [\[CrossRef\]](#)
20. Obot, I.B.; Ul-Haq, M.I.; Sorour, A.A.; Alanazi, N.M.; Al-Abeedi, T.M.; Ali, S.A.; Al-Muallem, H.A. Modified-Polyaspartic Acid Derivatives as Effective Corrosion Inhibitor for C1018 Steel in 3.5% NaCl Saturated CO₂ Brine Solution. *J. Taiwan Inst. Chem. Eng.* **2022**, *135*, 104393. [\[CrossRef\]](#)
21. Wang, L.; Gao, H.; Song, S.; Zhou, W.; Xue, N.; Nie, Y.; Feng, B. The Depressing Role of Sodium Alginate in the Flotation of Ca²⁺-Activated Quartz Using Fatty Acid Collector. *J. Mol. Liq.* **2021**, *343*, 117618. [\[CrossRef\]](#)
22. Wei, Q.; Jiao, F.; Dong, L.; Liu, X.; Qin, W. Selective Depression of Copper-Activated Sphalerite by Polyaspartic Acid during Chalcopyrite Flotation. *Trans. Nonferrous Met. Soc. China* **2021**, *31*, 1784–1795. [\[CrossRef\]](#)
23. Chen, C.; Sun, W.; Zhu, H.; Liu, R. A Novel Green Depressant for Flotation Separation of Scheelite from Calcite. *Trans. Nonferrous Met. Soc. China* **2021**, *31*, 2493–2500. [\[CrossRef\]](#)
24. Yang, L.; Li, Y.; Qian, B.; Hou, B. Polyaspartic Acid as a Corrosion Inhibitor for WE43 Magnesium Alloy. *J. Magnes. Alloys* **2015**, *3*, 47–51. [\[CrossRef\]](#)
25. Liu, Y.; Zhang, D.; Chen, C.; Zhang, J.; Cui, L. Adsorption Orientation of Sodium of Polyaspartic Acid Effect on Anodic Films Formed on Magnesium Alloy. *Appl. Surf. Sci.* **2011**, *257*, 7579–7585. [\[CrossRef\]](#)

26. Liu, C.; Ai, G.; Song, S. The Effect of Amino Trimethylene Phosphonic Acid on the Flotation Separation of Pentlandite from Lizardite. *Powder Technol.* **2018**, *336*, 527–532. [[CrossRef](#)]
27. Manouchehri, H.R. Pyrrhotite Flotation and Its Selectivity against Pentlandite in the Beneficiation of Nickeliferous Ores: An Electrochemistry Perspective. *Miner. Metall. Process.* **2014**, *31*, 115–125. [[CrossRef](#)]
28. Feng, B.; Feng, Q.; Lu, Y. The Effect of Lizardite Surface Characteristics on Pyrite Flotation. *Appl. Surf. Sci.* **2012**, *259*, 153–158. [[CrossRef](#)]
29. Zhang, L.; Guo, X.Y.; Tian, Q.H.; Li, D.; Zhong, S.P.; Qin, H. Improved Thiourea Leaching of Gold with Additives from Calcine by Mechanical Activation and Its Mechanism. *Miner. Eng.* **2022**, *178*, 107403. [[CrossRef](#)]
30. Liu, D.; Zhang, G.; Chen, Y.; Chen, W.; Gao, Y. A Novel Method to Limit the Adverse Effect of Fine Serpentine on the Flotation of Pyrite. *Minerals* **2018**, *8*, 582. [[CrossRef](#)]
31. Zhou, J.; Lu, Y.; Mao, G. Separation of Oxidized Pyrrhotite from Fine Fraction Serpentine. *Minerals* **2018**, *8*, 472. [[CrossRef](#)]
32. Liu, C.; Chen, Y.; Song, S.; Li, H. The Effect of Aluminum Ions on the Flotation Separation of Pentlandite from Lizardite. *Colloids Surf. A Physicochem. Eng. Asp.* **2018**, *555*, 708–712. [[CrossRef](#)]
33. Liu, D.; Zhang, G.; Li, B. Electrochemical and XPS Investigations on the Galvanic Interaction between Pentlandite and Pyrrhotite in Collectorless Flotation System. *Miner. Eng.* **2022**, *190*, 107916. [[CrossRef](#)]
34. Li, B.; Zhang, G.; Liu, D.; Chen, J. Selective Alteration Mechanisms of Sodium Tripolyphosphate towards Serpentine: Implications for Flotation of Pyrite from Serpentine. *J. Mol. Liq.* **2022**, *368*, 120687. [[CrossRef](#)]
35. Dong, L.; Jiao, F.; Qin, W.; Liu, W. Selective Flotation of Scheelite from Calcite Using Xanthan Gum as Depressant. *Miner. Eng.* **2019**, *138*, 14–23. [[CrossRef](#)]
36. Xie, T.; Yue, S.; Su, T.; Song, M.; Xu, W.; Xiao, Y.; Yang, Z.; Len, C.; Zhao, D. High Selective Oxidation of 5-Hydroxymethyl Furfural to 5-Hydroxymethyl-2-Furan Carboxylic Acid Using Ag-TiO₂. *Mol. Catal.* **2022**, *525*, 112353. [[CrossRef](#)]
37. Yang, S.; Xu, Y.; Liu, C.; Huang, L.; Huang, Z.; Li, H. The Anionic Flotation of Fluorite from Barite Using Gelatinized Starch as the Depressant. *Colloids Surf. A Physicochem. Eng. Asp.* **2020**, *597*, 124794. [[CrossRef](#)]
38. Boulton, A.; Fornasiero, D.; Ralston, J. Characterisation of Sphalerite and Pyrite Flotation Samples by XPS and ToF-SIMS. *Int. J. Miner. Process.* **2003**, *70*, 205–219. [[CrossRef](#)]
39. Chai, C.; Xu, Y.; Xu, Y.; Liu, S.; Zhang, L. Dopamine-Modified Polyaspartic Acid as a Green Corrosion Inhibitor for Mild Steel in Acid Solution. *Eur. Polym. J.* **2020**, *137*, 109946. [[CrossRef](#)]
40. Zhao, L.; Zhang, G.; Wang, M.; Zheng, S.; Li, B. Selective Separation of Smithsonite from Quartz by Using Sodium Polyaspartate as a Depressant. *Colloids Surf. A Physicochem. Eng. Asp.* **2022**, *644*, 128840. [[CrossRef](#)]
41. Wang, Y.; He, G.; Abudukade, D.; Li, K.; Guo, T.; Li, S.; Xiao, Z.; Wang, J.; Nie, S. Selective Inhibition of Sodium Tripolyphosphate on Calcite in the Process of Magnesite Flotation. *J. Mol. Liq.* **2022**, *345*, 117412. [[CrossRef](#)]
42. Bala, T.; Prasad, B.L.V.; Sastry, M.; Kahaly, M.U.; Waghmare, U.V. Interaction of Different Metal Ions with Carboxylic Acid Group: A Quantitative Study. *J. Phys. Chem. A* **2007**, *111*, 6183–6190. [[CrossRef](#)]
43. Tang, X.; Chen, Y. Using Oxalic Acid to Eliminate the Slime Coatings of Serpentine in Pyrite Flotation. *Miner. Eng.* **2020**, *149*, 106228. [[CrossRef](#)]
44. Liu, C.; Zheng, Y.; Yang, S.; Fu, W.; Chen, X. Exploration of a Novel Depressant Polyepoxysuccinic Acid for the Flotation Separation of Pentlandite from Lizardite Slimes. *Appl. Clay Sci.* **2021**, *202*, 105939. [[CrossRef](#)]